



UNIVERSITY OF LEEDS

This is a repository copy of *Turbulent Combustion Parameters in Gas Explosions with Two Obstacles with Variable Separation Distance*.

White Rose Research Online URL for this paper:

<http://eprints.whiterose.ac.uk/105090/>

Version: Accepted Version

Proceedings Paper:

Na'inna, AM, Phylaktou, HN and Andrews, GE orcid.org/0000-0002-8398-1363 (2016) Turbulent Combustion Parameters in Gas Explosions with Two Obstacles with Variable Separation Distance. In: Proceedings of the Eighth International Seminar on Fire & Explosion Hazards (ISFEH8). Eighth International Seminar on Fire & Explosion Hazards (ISFEH8), 25-28 Apr 2016, Hefi, China. USTC .

This is an author produced version of a paper published in Proceedings of the Eighth International Seminar on Fire & Explosion Hazards (ISFEH8). Uploaded in accordance with the publisher's self-archiving policy.

Reuse

Unless indicated otherwise, fulltext items are protected by copyright with all rights reserved. The copyright exception in section 29 of the Copyright, Designs and Patents Act 1988 allows the making of a single copy solely for the purpose of non-commercial research or private study within the limits of fair dealing. The publisher or other rights-holder may allow further reproduction and re-use of this version - refer to the White Rose Research Online record for this item. Where records identify the publisher as the copyright holder, users can verify any specific terms of use on the publisher's website.

Takedown

If you consider content in White Rose Research Online to be in breach of UK law, please notify us by emailing eprints@whiterose.ac.uk including the URL of the record and the reason for the withdrawal request.

Abdulmajid M. Na'inna , Herodotos N. Phylaktou, Gordon E. Andrews (2016).
Turbulent Combustion Parameters in Gas Explosions with Two Obstacles with Variable Separation Distance.
Proc. 8th International Seminar on Fire and Explosion Hazards, Hefei, China, April, 25-29, 2016.

Turbulent Combustion Parameters in Gas Explosions with Two Obstacles with Variable Separation Distance

Abdulmajid M. Na'inna ^{1*}, Herodotos N. Phylaktou ² Gordon E. Andrews ²

¹Nigerian Air Force, Abuja, Nigeria.

²Energy Research Institute University of Leeds, Leeds, United Kingdom.

*Corresponding author email:

amnainna@gmail.com/profgeandrews@hotmail.com/h.n.phylaktou@leeds.ac.uk

ABSTRACT

Most of the congested gas explosions studies have focused on quantifying global flame acceleration and maximum overpressure through obstacle groupings rather than detailed analysis of the flame propagation through the individual elements of the congested region. Fundamental data of the turbulent flow and combustion parameters would aid better understanding of gas explosion phenomena and mechanisms in the presence of obstacles in addition to the traditional flame speeds and overpressures that are usually reported. In this work we report near stoichiometric methane/air explosion tests in an elongated vented cylindrical vessel 162 mm internal diameter with an overall length-to-diameter, L/D of 27.7. Single and double obstacles (both hole and flat-bar types) of 20-40% blockage ratios, BR with variable obstacle scale were used. The spacing between the obstacles was systematically varied from 0.5 m to 2.75 m. Turbulence parameters were estimated from pressure differential measurements and geometrical obstacle dimensions. This enabled the calculation of the explosions induced gas velocities, rms turbulent velocity, turbulent Reynolds number and Karlovitz number. This allowed the current data to be plotted on a premixed turbulent combustion regimes diagram. The bulk of the data fell in the thickened-wrinkled flames regime. The influence of the calculated Karlovitz number on the measured overpressures was analysed and was related to obstacle separation distance and obstacle scale characteristics.

KEYWORDS: Gas explosions, Turbulent combustion parameters, Obstacle separation distance

INTRODUCTION

Most of the congested gas explosions studies have focussed on quantifying global flame acceleration and maximum overpressure through obstacle groupings rather than detailed analysis of the flame propagation through the individual elements of the congested region. Fundamental turbulent parameters such as intensity of turbulence, u'/U , turbulent Reynolds number, R_ℓ Karlovitz number, K_a , turbulent flame speed, S_T etc. would aid better understanding of gas explosion dynamics in the presence of obstacles but such data are difficult to obtain experimentally [1-2]. The transient nature of obstacle induced explosion flow coupled with the harshness of the event when they are at realistic turbulence levels make such measurements difficult and expensive.

Data from cold flow turbulence induced by grid plates were used to predict the maximum u'/U where the maximum explosion severity occurs [3]. However, the transient combustion parameters measured by the few researchers were based on single obstacle gas explosions; even though, typical gas explosions in industries do occur in multi-obstacle situations. In multi-obstacle gas explosions, the spacing between obstacles is an important factor that determines the severity of such explosions in terms of flame speeds and overpressures [4-7]. It was the aim of this work to measure turbulence combustion parameters from transient gas explosions with obstacles of varying obstacle spacing.

EXPERIMENTAL

A long cylindrical vessel 162 mm internal diameter made from nine flanged sections, 8 of them of 0.5 m length each and one section 0.25m in length (total nominal length of 4.25m). The test vessel was rated to withstand an overpressure of 35 bar. It was mounted horizontally and closed at the ignition end, with its open end connected to a large cylindrical dump-vessel with a volume of 50 m^3 . This arrangement enabled the simulation of open-to-atmosphere explosions with accurate control of both test and dump vessels pre-ignition conditions.

Single and double obstacles (both hole and flat-bar types) made from stainless steel of 3.2 mm thick, and 20 - 40% blockage ratio, BR were used in the test vessel to generate turbulence. The difference in obstacle BR achieved a variation of the obstacle scale, b. The width of the flat-bar obstacles is taken to be the b. For the hole – type obstacles, the b was considered to be the nominal width of the solid material between holes using the same definition given in Baines and Peterson [8] for multi-hole grids, based on notional large grid plate with multiple holes of size and BR equal to the single hole actual obstacle, given as,

$$b = D - 0.95d \quad (1)$$

D and d in Eq. 1 are the internal tube diameter and the obstacle-hole diameter respectively. The obstacles as shown in Fig. 1 were mounted between the section flanges. For the double obstacle tests, the first obstacle was positioned 1 m downstream of the spark (for all tests) while the second obstacle's position was varied from 0.5 m to 2.75 m downstream of the first obstacle in order to obtain the worst case obstacle spacing.



Figure 1. Turbulent generating obstacles – hole type (left), flat bar type (right).

A pneumatically actuated gate valve isolated the test vessel prior to mixture preparation. A vacuum pump was used to evacuate the test vessel before a 10 % methane-air mixture by volume (with 0.45 m/s laminar burning velocity, S_L) was formed using partial pressures, to a total mixture pressure of 1 atm. The dump vessel was filled with air to a pressure of 1 atm as well. After mixture circulation, allowing for at least 4 volume changes, the gate valve to the dump vessel was opened and a 16 Joule spark plug ignition was effected at the centre of the test vessel closed-end flange. The test vessel had an overall length-to-diameter ratio, L/D of 27.7. The set-up is shown in Fig. 2.

An array of 24 type-K mineral insulated exposed junction thermocouples positioned along the axial centre line of the test vessel was used to record the time of flame arrival. Average flame speeds allocated to the midway position between two thermocouples were obtained by dividing the distance between two thermocouples by the difference in time of flame arrival at each thermocouple position. A smoothing algorithm was applied to the flame arrival data, as described by Gardner [2], to avoid either high or negative flame speeds where the flame brush appears to arrive at downstream centreline locations earlier than upstream ones. This is particularly in the regions of strong acceleration downstream of the obstacles. The test vessel and dump vessel pressure histories were recorded using an array of 8 Keller type pressure transducers - 7 gauge pressure transducers (PT1to PT7) and 1 differential (DPT), as shown in Fig. 2. Wall static pressure tapping measured by a differential pressure transducer (DPT) were located at 1D upstream and 0.5D downstream of the first obstacle as specified in British Standard [9]. Pressure transducers, PT3 and PT4 were positioned 1D upstream and 0.5D downstream of the second obstacle and they were used to obtain the pressure differential, ΔP_d across these obstacles and were used in calculating the induced gas flow velocities, S_g and other flow turbulence characteristics. Pressure transducers PT1 and PT6 were positioned permanently at the ignition position-end flange and end of the test vessel (25D from the spark) respectively. The pressure history in the dump vessel was measured using PT7 positioned as shown in Fig.2.

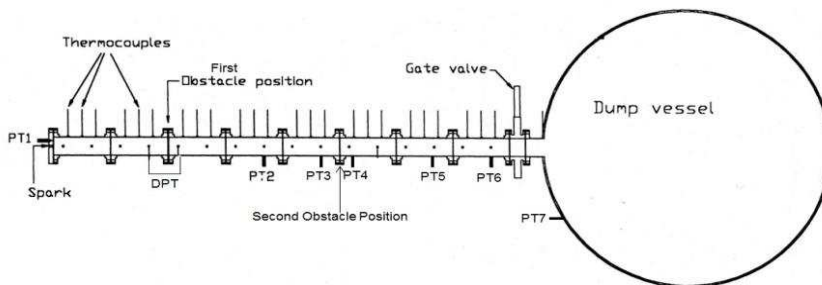


Figure 2. Schematic diagram of the experimental set up.

A 32-channel (maximum sampling frequency of 200 KHz per channel) transient data recorder (Data Logger and FAMOS) was used to record and process the explosion data. Each test was repeated at least three times. In presenting the results of the experimental tests in this research, all the repeat tests were shown on the graph where possible. However, for clarity purposes average results are shown in some cases for the analysis of the turbulent parameters. In total, over 72 tests were carried out demonstrating 24 different test conditions. Table 1 shows a list of the tests carried out as part of this work.

Table 1. Summary of the experimental tests conditions.

Test (-)	Shape (-)	BR (-)	K (-)	No (-)	N _h /b (-)	b (m)	x _s /b (-)		
1			No obstacle						
2	Hole	0.3	0.76	1	1	0.033	-		
3	Hole	0.3	0.76	2	1	0.033	15.0		
4	Hole	0.3	0.76	2	1	0.033	30.1		
5	Hole	0.3	0.76	2	1	0.033	37.6		
6	Hole	0.3	0.76	2	1	0.033	52.7		
7	Hole	0.3	0.76	2	1	0.033	67.7		
8	Hole	0.3	0.76	2	1	0.033	82.7		
9	Hole	0.4	1.80	1	1	0.043	-		
10	Hole	0.4	1.80	2	1	0.043	29.2		
11	Hole	0.4	1.80	2	1	0.043	34.9		
12	Hole	0.4	1.80	2	1	0.043	52.6		
13	Hole	0.2	0.26	1	1	0.024	-		
14	Hole	0.2	0.26	2	1	0.024	71.9		
15	Hole	0.2	0.26	2	1	0.024	92.4		
16	Hole	0.2	0.26	2	1	0.024	112.9		
17	Bar	0.2	0.26	1	1	0.026	-		
18	Bar	0.2	0.26	2	1	0.026	68.4		
19	Bar	0.2	0.26	2	1	0.026	87.9		
20	Bar	0.2	0.26	2	1	0.026	107.4		
21	Bar	0.3	0.76	1	1	0.039	-		
22	Bar	0.3	0.76	2	1	0.039	32.5		
23	Bar	0.3	0.76	2	1	0.039	45.5		
24	Bar	0.3	0.76	2	1	0.039	58.4		

K = Obstacle pressure loss coefficient, Nh/b = Number of hole/bar obstacle Xs = obstacle separation

RESULTS AND DISCUSSIONS

Explosion Induced Gas Velocities

By considering the obstacle as an orifice plate and using the procedures described in the British Standard [9], the maximum unburnt gas flow velocity ahead of the flame was calculated from the experimental measured static pressure difference across the obstacle using static pressure tappings at 1D and 0.5D upstream and downstream of the obstacle respectively. It is worth noting that the Standard is meant for flow calculations in steady state conditions and not for a transient as in the present application. However, Phylaktou and Andrews [3] established the applicability of steady-state flow to congested gas explosions.

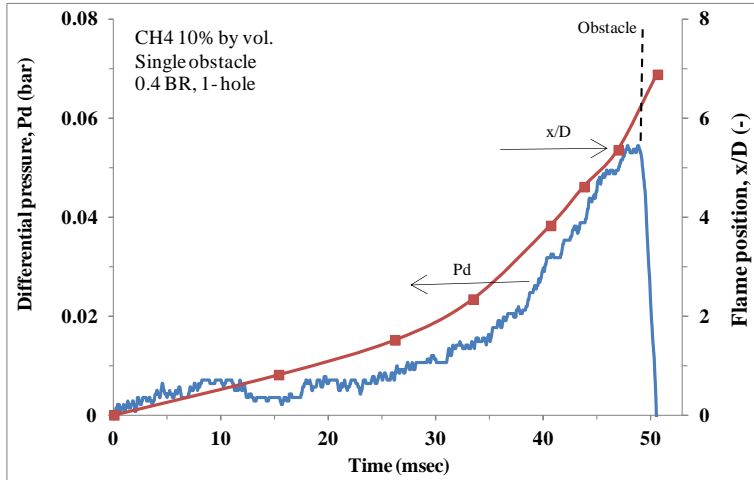


Figure 3. Measured pressure drop across a single 1-hole obstacle.

The measurement of ΔP_d due to single 1-hole obstacle of 0.4 BR with 10% CH₄ by vol. was obtained from the recorded differential pressure trace as shown in Fig. 3. Also shown is the flame position up to its arrival at the last thermocouple prior to the obstacle. The ΔP_d increased as the flame propagated towards the obstacle. As the flame reached the obstacle, the forced flow through the obstacle (and therefore the turbulence generation) terminated. This led to an abrupt drop in pressure, ΔP_d , across the obstacle. This happened at a point just after flame arrival was recorded at the last thermocouple (TC6) before the obstacle. The location of the maximum ΔP_d therefore signified the time of flame arrival at the obstacle and was the period of maximum flow velocity through the obstacle. This shows that the significance of pressure loss caused by friction was negligible compared to that due to flow interaction with the obstacle, as the measurement point for ΔP_d behind the obstacle was in close proximity to the obstacle. A similar trend was obtained for ΔP_d across the second obstacles with higher pressure drop compared to that of first obstacle. The pressure loss in this case was obtained by finding the difference between the pressure trace from pressure transducer PT3 and PT4 for the second obstacle.

For all the obstacle types used in the current work, the ΔP_d was used in the calculation of mass flow rate, \dot{m} using the calculation procedure in the British Standard [9].

By considering the area of the tube, A , and the density, ρ (for the actual system pressure in the vicinity of the flame just before going through the obstacle), S_g is thus given as,

$$S_g = \frac{\dot{m}}{\rho A} \quad (2)$$

Maximum r.m.s. Turbulent Velocity

The maximum intensity of turbulence, u'/U_{\max} leading to maximum severity in explosions was obtained by Phylaktou and Andrews [3] as,

$$u'/U_{\max} = C_T K^{0.5} \quad (3)$$

C_T and K are defined as the turbulence generation constant and pressure loss coefficient respectively. For thin/sharp (thickness/diameter, $t/d < 0.6$) obstacle used in this work, C_T is 0.225 whereas K for a given porosity ratio, p ($p = 1 - BR$) is given in Eqn 4 as,

$$K = \left[\frac{1}{p[0.872 - 0.015(\frac{t}{d}) - 0.08(d/t)](1-p^{3.3}) + p^{4.3}[1+0.134(t/d)^{0.5}]^{-1}} - 1 \right]^2 \quad (4)$$

Table 2 gives an overview of all the maximum u' calculated in the current research for a given mean flow velocity, U (assumed to be S_g in the current work). Also presented are the other turbulent combustion parameters (to be discussed later) such as R_ℓ , S_T and K_a amongst others.

Table 2. Summary of the calculated turbulent combustion parameters

Test (-)	ΔP_s (Pa)	$S_{g(\max)}$ (m/s)	u/S_L (-)	R_ℓ (-)	S_T (m/s)	K_a (-)	ℓ/δ_ℓ (-)
1					No obstacle		
2	5900	41	18	9390	20	0.52	522
3	22333	80	35	18416	34	1.40	533
4	62333	114	50	35981	49	2.03	726
5	83000	132	58	41236	55	2.56	716
6	106667	153	67	45793	61	3.26	687
7	56667	116	50	32078	48	2.23	636
8	19000	64	28	19330	31	0.88	693
9	5333	34	23	14952	26	0.66	660
10	124000	138	93	85532	86	4.63	922
11	152000	160	107	90888	94	5.97	849
12	104000	128	86	77637	81	4.14	905
13	8833	58	15	5606	16	0.46	380
14	29797	98	25	11115	25	0.94	442
15	19083	79	20	8866	21	0.68	440
16	43312	124	32	12827	29	1.39	405
17	9765	55	14	5314	15	0.43	377
18	32393	89	23	11024	24	0.77	485
19	57473	118	30	14722	30	1.18	488
20	47327	111	28	12893	28	1.11	454
21	14420	53	23	13814	26	0.73	592
22	86390	109	47	40871	50	1.75	862
23	106000	117	51	46620	54	1.90	913
24	51433	90	39	29529	41	1.40	754

Turbulent Reynolds Number

Most of the real combustion systems operate in turbulent regimes with values of R_ℓ ranging from 250 to 25,000 [10]. For instance, the estimated R_ℓ value for a bunsen burner was found to be 1,500 whereas a gas turbine combustion chamber operating at maximum power has R_ℓ higher than that of the bunsen burner by 13.3 folds. Ironically, most studies on experimental flame structure do not characterize systems of practical concern, because they have been performed in regimes with R_ℓ well below 250 and this is more accurately referred to as trivial turbulence levels. The problem is that most models on turbulent combustions are intended at predicting these trivial turbulent flames [1]. In vapour cloud explosions with pipe arrays, Catlin and Johnson [11] estimated R_ℓ in the order of 70,000. AbdelGayed and Bradley [12] estimated that atmospheric explosions can be related with R_ℓ values in the range of 10^6 to 10^7 . For a given u' , integral length scale, ℓ ($\ell = 0.5b$) and kinematic viscosity, v ; the R_ℓ in the present work is calculated as,

$$R_\ell = (u' \ell / v) \quad (5)$$

As observed from other turbulent combustion parameters, R_ℓ for the single obstacles (30% BR 1-hole) were similar for all separations with a value of close to 10,000. This is well within turbulent flow regime. For the double obstacle tests, R_ℓ was found to change with pitch. The maximum value of R_ℓ with the double obstacle at 1.75 m apart was close to 50,000. This value

was nearly five folds higher than the single obstacle and doubled that of two obstacles separated at 0.5 m and 2.75 m.

All the R_ℓ obtained in the present research (see Table 2) were above 4000 i.e. cut off value for turbulence. A maximum value of over 90,000 was realised for test 11. This was due to the influence of high u' induced by fast combustion-generated flow through the obstacles and the integral length scale, ℓ which is dependent on obstacle scale, b . Therefore this suggests that the current experiments are of direct application to real systems.

Turbulent Burning Velocity

Assuming a 1-D flame propagation (spherical or planar flame moving for example from the closed ignition end of the tube towards the open end of the tube), the flame speed, S_f is greater than the burning velocity, S_u (either laminar or turbulent) due to the expansion of the burnt gases behind the flame front, E . The interaction of a flame with an obstacle results in an increase of the flame area. The flame shape distorts as it follows the turbulent flow patterns downstream of the obstacle. The turbulent burning velocity, S_T that results is therefore greater than the laminar value, S_L . Assuming an adiabatic condition (with no heat loss), the S_T is given as the ratio of $S_{f\max}$ to E ($E = 7.5$ for 10% CH₄ by vol.). The $S_{f\max}$ for the tests in this work were obtained from the previous work of the authors [4-7]. However, in the present study, the S_T is calculated using Eq 6 as given by Phylaktou [1]. Figure 4 shows a plot of S_T from [1] against that under adiabatic conditions with an R^2 value of 85% indicating a very good agreement.

$$\frac{S_T}{S_L} = 1 + 0.67 \left(\frac{u'}{S_L} \right)^{0.47} R_i^{0.31} \quad (6)$$

Karlovitz Number and Flame Quenching

Karlovitz[13] quantified that for turbulent flames, the flame straining is expressed by the Karlovitz stretch factor otherwise known as Karlovitz number, Ka as the ratio of the chemical lifetime to the turbulent lifetime. Abdel-Gayed et al. [14] further defined Ka based on turbulent Reynolds number, R_ℓ with dependence on ℓ as,

$$Ka = 0.157 \left(\frac{u'}{S_L} \right)^2 R_\ell^{-0.5} \quad (7)$$

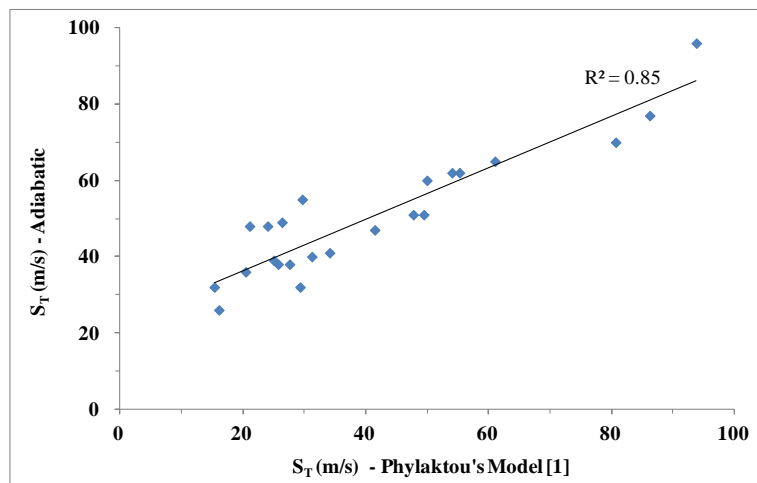


Figure 4. A Plot of S_T correlation under adiabatic condition and that given by Phylaktou [1].

At sufficiently high turbulence levels, flame front fragmentation can result in partial or full quenching of the flame [15]. Global quenching of premixed flames is of both fundamental and practical importance. As the premixed flame encounters external perturbations like heat loses or aerodynamic stretch, quenching of the flame may take place provided the perturbations are strong enough to diminish the reaction rate in the flame to an insignificant value [16].

For a stoichiometric methane-air mixture, flame quenching was estimated for values of Ka above 1.5. Later correlations presented by Abdel-Gayed et al. [17] proposed flame quench for $Ka \geq 1$. Further study on flame extinction by Bradley et al. [18] showed that Eq. 7 corresponded to the lower boundary of the quenching process; hence the new quench limit was extended to $Ka \geq 6$.

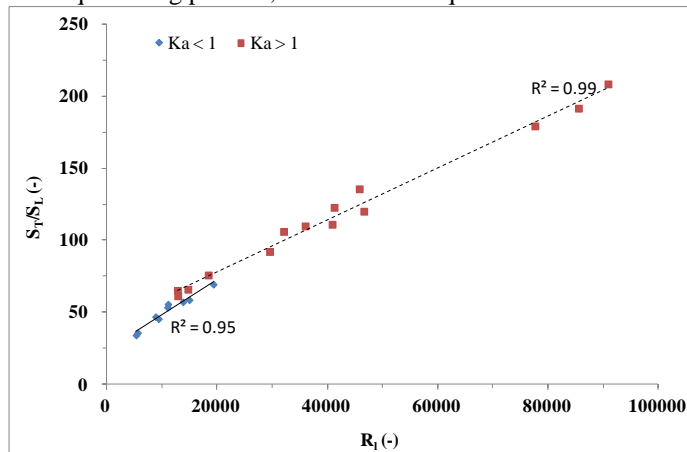


Figure 5. Relationship between turbulent burning velocity and the turbulent Reynolds number.

Figure 5 shows a strong relationship between the turbulent Reynolds number and turbulent burning velocity for $Ka < 1$ and $Ka > 1$ with both having close to 100% agreement. A turbulent Reynolds number of over 90,000 was obtained at a Ka value of over unity corresponding to S_T/S_L of about 210. For data set with Ka value of below unity on the other hand, a turbulent Reynolds number of about 20,000 was measured. This value is about 4.5 times lower than the R_ℓ of $Ka > 1$. However, an S_T/S_L of 70 which is three folds lesser than that of $Ka > 1$ was realised. This analysis of Fig 5 further reiterates that tests with $Ka > 1$ are associated with very high turbulent flows and in some cases (though not in this work) leading to flame fragmentation and quenching.

The scale of importance in turbulent combustion is not the whole size of the rig but rather the size of the turbulent generator as this determines the length scale, ℓ . In explosions the turbulence initiators are the obstacles and for grid plate obstacle or similar the dimension that defines ℓ is the width of the solid materials between the holes. From Table 1, three sets of fairly similar ℓ ($\ell = 0.5b$) for all the obstacles exist. Set 1 ranges from 12 – 13 mm, 17 mm for set 2 and set 3 spans from 19 – 21 mm. However, data from set 2 was merged with that of set 3 due to data insufficiency. Figure 6 shows a plot of S_T/S_L against Ka for 2 sets of scales (set 1, 12mm – 13 mm and set 2, 17mm – 21mm). For all sets of ℓ , the Ka was found to increase with increase in S_T/S_L with over 90% agreement. Furthermore, ℓ from set 2 attained a maximum value of 6 for Ka which corresponds to S_T/S_L of about 210. These values are about 5 and 2 times higher than those ℓ from set 1 for Ka and S_T/S_L respectively.

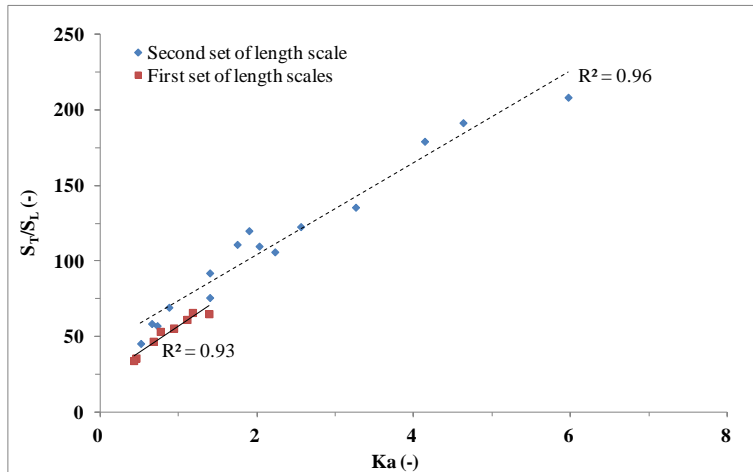


Figure 6. Relationship between turbulent burning velocity and the Karlovitz number.

Turbulent Premixed Combustion Regimes

Premixed turbulent combustion regimes could be related to turbulence and chemical characteristic length and time scales. This investigation leads to combustion diagrams where different regimes are given as function of non-dimensional numbers [19-23]. The diagrams could serve as a guide to choose and develop the appropriate combustion model for a specified situation.

Figure 7 shows the various regimes of turbulent premixed combustion as specified in [22-23] using the length scale (ℓ/δ_ℓ) and the velocity (u'/S_L) ratios. The flame thickness, δ_ℓ is taken to be the ratio of the kinematic viscosity, ν to S_L . A Klimov-Williams criterion for Ka equals to unity is attained when the δ_ℓ is equivalent to the Kolmogorov length scale, η . Below this line, the flame is thinner than any turbulent length scales. Below the line delineating the Peters criterion i.e. $Ka = 100$, the thickness of the reaction zone is thinner than any turbulent length scales and is not influenced by turbulent motions. In the present experiments, the dimensionless ratios (ℓ/δ_ℓ and u'/S_L) were calculated and listed in Table 2 and plotted on Fig. 7. It can be seen that the data points fall in the thickened-wrinkled flames regime. Previous researchers have presented their turbulent combustion regimes using Borghi diagrams and showed that most of the explosion data were in the distributed reaction zone [1-2].

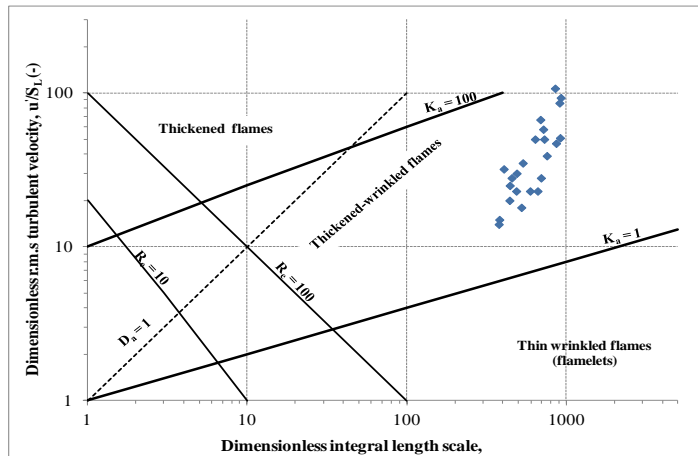


Figure 7. Present research data on premixed turbulent combustion regimes diagram as specified in Peters [22-23].

CONCLUSION

Turbulence parameters were estimated from pressure differential measurements and geometrical obstacle dimensions. This enabled the calculation of the explosions induced gas velocities, r.m.s, S_g , turbulent velocity, S_T , turbulent Reynolds number, R_f and Karlovitz number, K_a . A complete turbulence profile similar to that of overpressure and flame speeds profiles was formed with all the turbulent combustion parameters predicted in this research as a function of the obstacle separation distance.

All the R_f obtained in the present work were above the cut off value for turbulent flow with a maximum value of over 90,000. This was due to the influence of high u' induced by fast combustion-generated flow through the obstacles and the integral length scale, ℓ which is dependent on obstacle scale, b . Therefore this suggests that the current experiments are of direct application to real systems. Additionally, a high S_T value of about 94 m/s was realized using an S_T model correlation from the literature. For most of the single obstacle tests, K_a value of below unity signifying no flame quenching was realized. However, K_a value of greater than unity was realised with the double obstacle tests. Theoretically, K_a above unity indicates global flame extinction however, the entire flame quench was not observed in any of the present tests. In all cases the explosion propagated strongly, leading to significant overpressures. The values of K_a in this study would therefore suggest a measure of the prevailing flame straining conditions downstream of an obstacle, as opposed to an indication of flame extinction. The present research data were presented on the recent premixed turbulent combustion regimes diagram and the bulk of the data points fall in the thickened-wrinkled flames regime. The turbulent motions in this regime are capable of affecting and thickening the flame preheat zone, but not able to change the reaction zone which still remains thin and near to a laminar reaction zone.

REFERENCES

1. Phylaktou, H. N., "Gas Explosions In Long Closed Vessels With Obstacles : A Turbulent Combustion Study Applicable to Industrial Explosions". PhD Thesis, University of Leeds, 1993.
2. Gardner, C. L. 1998. "Turbulent Combustion in Obstacle-Accelerated Gas Explosions – The Influence Of Scale". PhD Thesis, University of Leeds, 1998.

3. Phylaktou, H. N., and Andrews G. E., "Prediction of the maximum turbulence intensities generated by grid-plate obstacles in explosion-induced flows," *Symposium (International) on Combustion*, **25**:103-110 (1994).
4. Na'inna, A.M., Phylaktou H.N., Andrews, G.E., "The Acceleration Of Flames In Tube Explosions With Two Obstacles As A Function Of The Obstacle Separation Distance," *Journal Of Loss Prevention In The Process Industries*, **26**: 1597-1603 (2013).
5. Na'inna, A.M., Phylaktou, H., and Andrews, G.E., "Acceleration of Flames in Tube Explosions with Two Obstacles as a Function of the Obstacle Separation Distance: The Influence of Mixture Reactivity," in: Proc. of the Seventh International Seminar on Fire and Explosion Hazards (ISFEH7), Research Publishing, Providence, USA, 2013, pp. 627-636.
6. Na'inna, A.M., Phylaktou, H.N. and Andrews, G.E., "Effects of obstacle separation distance on gas explosions: the influence of obstacle blockage ratio," *Procedia Engineering* **84**: 306 – 319 (2014).
7. Na'inna, A.M., Somuano, G.B., Phylaktou, H.N., and Andrews G.E., "Flame acceleration in tube explosions with up to three flat-bar obstacles with variable obstacle separation distance," *Journal of Loss Prevention in the Process Industries* **38**: 119-124 (2015).
8. Baines, W. D. and Peterson, E. G., 1951. "An investigation of flow through screens," *Trans. American Society of Mechanical Engineering*, **73**:167 (1951).
9. BS5167-2., "Measurement of fluid flow by means of pressure differential devices inserted in circular cross-section conduits running full - Part 2: Orifice plates." 2003.
10. Andrews, G. E., Bradley, D. and Lwakabamba, S. B., "Turbulence and turbulent flame propagation-A Critical Appraisal," *Combustion and Flame*, **24**:285-304 (1975).
11. Catlin, C. A. and Johnson, D. M., "Experimental scaling of the flame acceleration phase of an explosion by changing fuel gas reactivity," *Combustion and Flame*, **88**:15-27 (1992).
12. Abdel-Gayed, R. G. and Bradley, D., "The influence of turbulence upon the rate of turbulent burning, In Fuel Air Explosions [manuscript]. At: University of Waterloo Press, Montreal, p.51. 1982
13. Karlovitz, B. 1954. Selected Combustion Problems. London: Butterworths. 1954, p.248.
14. Abdel-Gayed, R. G., Al-Khishali, K. J. and Bradley, D., "Turbulent Burning Velocities and Flame Straining in Explosions," *Proceedings of the Royal Society of London. A. Mathematical and Physical Sciences*, **391**:393-414 (1984).
15. Abdel-Gayed, R. G. and Bradley, D., "Criteria for turbulent propagation limits of premixed flames," *Combustion and Flame*, **62**: 61-68 (1985).
16. Yang, S. I. and Shy, S. S., "Global quenching of premixed CH₄/air flames: Effects of turbulent straining, equivalence ratio, and radiative heat loss," *Proceedings of the Combustion Institute*, **29**(2), 1841-1847 (2002).
17. Abdel-Gayed, R. G., Bradley, D., Hamid, M. N., and Lawes, M., "Lewis number effects on turbulent burning velocity," *Symposium (International) on Combustion*, **20**:505-512 (1985).
18. Bradley, D., Lau, A. K. C., and Lawes, M., "Flame Stretch Rate as a Determinant of Turbulent Burning Velocity," *Philosophical Transactions of the Royal Society of London. Series A: Physical and Engineering Sciences*, **338**:359-387 (1992).
19. Williams, F. E. ed. *Combustion theory*. Addison-Wesley, 1985.
20. Borghi, R., "Turbulent combustion modelling," *Progress in Energy and Combustion Science*, **14**:245-292 (1988).
21. Peters, N., "Laminar flamelet concepts in turbulent combustion," *Symposium (International) on Combustion*, **21**:1231-1250 (1988).
22. Borghi, R. and Destriau, M., eds. *Combustion and flames, chemical and physical principles*. Paris: Editions Technip, 1998.
23. Peters, N., "The turbulent burning velocity for large-scale and small-scale turbulence," *Journal of Fluid Mechanics*, **384**:107-132 (1999).